The Journal of Immunology

Antitumor Activity of IFN-λ in Murine Tumor Models

Atsuko Sato, Mamitaro Ohtsuki, Megumi Hata, Eiji Kobayashi and Takashi Murakami

J Immunol 2006; 176:7686-7694; ;
doi: 10.4049/jimmunol.176.12.7686
http://www.jimmunol.org/content/176/12/7686

The Journal of Immunology is published twice each month by
The American Association of Immunologists, Inc.,
1451 Rockville Pike, Suite 650, Rockville, MD 20852

Print ISSN: 0022-1767 Online ISSN: 1550-6606.

Antitumor Activity of IFN-λ in Murine Tumor Models[1]

Atsuko Sato,*† Mamitaro Ohtsuki,† Megumi Hata,* Eiji Kobayashi,* and Takashi Murakami[2]*

IFN-λ 1, -λ 2 and -λ 3 have been discovered as the latest members of the class II cytokine family and shown to possess antiviral activity. Murine B16 melanoma and Colon26 cancer cells were transduced with mouse IFN-λ to determine whether IFN-λ possesses antitumor activity. Overexpression of IFN-λ induced cell surface MHC class I expression and Fas/CD95 Ag, induced significant caspase-3/7 activity, and increased $p21^{Waf1/Cip1}$ and dephosphorylated Rb (Ser^{780}) in B16 cells in vitro. IFN-λ expression in tumor cell lines markedly inhibited s.c. and metastatic tumor formation in vivo compared with mock transfections ($p < 0.05$). Moreover, IFN-λ expression induced lymphocytic infiltrates, and an Ab-mediated immune cell depletion assay showed that NK cells were critical to IFN-λ-mediated tumor growth inhibition. Hydrodynamic injection of IFN-λ cDNA successfully targeted liver metastatic foci of Colon26 cells, and moderately decreased the mortality of mice with tumors. IFN-λ overexpression in the liver increased NK/NKT cells and enhanced their tumor-killing activity, and suggested the activation of innate immune responses. Thus, IFN-λ induced both tumor apoptosis and NK cell-mediated immunological tumor destruction through innate immune responses. These findings suggested that local delivery of IFN-λ might prove a useful adjunctive strategy in the clinical treatment of human malignancies. ***The Journal of Immunology,*** **2006, 176: 7686–7694.**

Advances in cancer treatment include the introduction of chemotherapeutic regimens, novel vaccination strategies, and cytokine therapies (1–5). Cytokines, including the IFNs, play a critical role in modulating innate and adaptive immune systems (6, 7). The IFN family is divided into type I and type II IFNs (8). The type I group contains at least 13 IFN-α members, IFN-β and IFN-ω in humans, whereas the type II group is represented by the single member IFN-γ. Type I IFNs modulate the adaptive immune response by increasing MHC class I expression to promote Ag presentation (9), enhance T cell survival (10), and stimulate dendritic cell (DC)[3] maturation (7, 11). In fact, certain type I IFNs have been approved for use in clinical oncology involving hairy cell leukemia, malignant melanoma, and AIDS-related Kaposi's sarcoma (12). Notwithstanding these applications, patients undergoing IFN therapy often only have a limited response, and most have adverse effects that include fatigue, fever, and anorexia (13). Consequently, improved alternative therapies are required for clinical applications.

IFN-λ1, -λ2, and -λ3 (also referred to as IL-29, IL-28a, and IL-28b) were identified as the latest members of the class II cytokine family following computational analysis of the human genomic sequence (14, 15). Although these new IFNs share limited sequence similarity to type I IFNs, they are expressed by PBMC and DCs following viral infection or stimulation with poly(I:C) (14, 15), and have been shown to possess antiviral activity similar to type I IFNs (14–17). They bind to the common IL-28R (also referred to as CRF2–12, LICR2, and IFN-λR1), which associates with IL-10Rβ and serves as a high-affinity binding complex for IFN-λs (14–16). The heterodimeric receptor mediates JAK1 activation and tyrosine phosphorylation of STAT factors (15, 16), leading to biological responses similar to those elicited by type I IFNs. The similar mode of action between IFN-λ and type I IFNs suggested that IFN-λs might possess antitumor activity.

In a previous study concerning the development of immunization strategies, we demonstrated that use of naked plasmid DNA has considerable potential to modulate humoral and cellular immune responses that protect against cancer and infectious diseases (18–22). Specifically, i.v. injection with a large volume of plasmid DNA solution (referred to as the hydrodynamic injection method) can result in preferential gene expression in the liver of rodents (23–26). The hydrodynamic method potentially allows for liver-selective gene delivery to target metastatic foci.

In this study, we examined the antitumor activity of mouse IFN-λ with respect to murine tumors. Murine melanoma B16 and colon cancer Colon26 cell lines expressed functional IFN-λ receptors, and transient transduction using mouse IFN-λ cDNA into B16 cells enhanced MHC class I expression and the appearance of cell surface Fas (CD95) Ag. Overproduction of IFN-λ suppressed cell proliferation in vitro by inducing $p21^{Waf1/Cip1}$ and dephosphorylated Rb (Ser^{780}), and resulted in increased caspase-3/7 activity. This suggested the induction of apoptotic cell death concomitant with cell cycle arrest. Furthermore, local overproduction of IFN-λ also inhibited s.c. and metastatic tumor growth in vivo. Therapeutic injection of naked IFN-λ cDNA by hydrodynamic injection targeted liver metastatic foci of Colon26 cells by increasing the number of NK/NKT cells. Ab-mediated depletion of immune cells supported the notion that the in vivo antitumor activity of IFN-λ is dependent on a NK cell-mediated tumor destruction pathway. These results demonstrated that local delivery of IFN-λ induced both tumor apoptosis and NK cell-mediated immunological tumor destruction. Therefore, we propose that use of IFN-λ might prove a useful adjunctive strategy in the clinical treatment of human malignancies.

*Division of Organ Replacement Research, Center for Molecular Medicine, Jichi Medical School, Shimotsuke, Tochigi, Japan; and †Department of Dermatology, Jichi Medical School, Shimotsuke, Tochigi, Japan

Received for publication October 17, 2005. Accepted for publication March 31, 2006.

The costs of publication of this article were defrayed in part by the payment of page charges. This article must therefore be hereby marked *advertisement* in accordance with 18 U.S.C. Section 1734 solely to indicate this fact.

[1] This study was supported by a grant to T.M. from the Kowa Life Science Foundation and the Ministry of Education, Culture, Sports, Science and Technology (MEXT) of Japan (Project No. 17591181), and by a grant to E.K. from the High-Tech Research Center Project for Private Universities: matching fund subsidy, and the Center of Excellence Program from MEXT.

[2] Address correspondence and reprint requests to Dr. Takashi Murakami, Division of Organ Replacement Research, Center for Molecular Medicine, Jichi Medical School, 3311-1 Yakushiji, Shimotsuke, Tochigi 329-0498, Japan. E-mail address: takmu@jichi.ac.jp

[3] Abbreviations used in this paper: DC, dendritic cell; EGFP, enhanced GFP.

0022-1767/06/$02.00

Materials and Methods

Animals, cells, and reagents

Male C57BL/6J and BALB/c mice (8–12 wk old) were purchased from Charles River Japan. All experiments in this study were performed in accordance with the Jichi Medical School Guide for Laboratory Animals.

B16/F0, B16/F10, NIH3T3, L929, and COS7 cells were maintained in DMEM (Invitrogen Life Technologies) with 10% heat-inactivated FCS and supplements (27). Colon26, EL-4, and P815 cells were grown in RPMI 1640 (Invitrogen Life Technologies) with 10% FCS and supplements. The cultures were kept in a 5% CO_2 and 95% air-humidified atmosphere at 37°C. Depleting anti-CD4 (clone GK1.5, rat IgG2b) and anti-CD8 (clone 2.43, rat IgG2b) mAb-producing hybridoma cells were obtained from the American Type Culture Collection.

Anti-phospho-Rb (Ser^{780}) (Cell Signaling Technology), anti-mouse $p21^{Waf1/Cip1}$ (BD Pharmingen), and anti-actin (sc-1616; Santa Cruz Biotechnology) Abs were used for Western blotting. For the FLAG-tagged IFN-λ, anti-FLAG M2 mAb (Sigma-Aldrich) was used. For the flow cytometric analysis, PE-conjugated anti-mouse H-$2K^b$ mAb, PE-conjugated anti-mouse Fas mAb, PE-conjugated anti-mouse NK1.1 mAb, FITC-conjugated anti-mouse CD3ε mAb, and isotype-matched IgG controls were purchased from BD Pharmingen. FITC-conjugated anti-mouse H-$2K^k$ mAb was obtained from Miltenyi Biotec.

RT-PCR and mouse IFN-λ cDNA cloning

Total RNA was extracted from cells using Isogen (Nippon Gene). Two micrograms of total RNA was used for first-strand synthesis using SuperScript III reverse transcriptase (Invitrogen Life Technologies). PCR was then performed using Platinum *Pfx* polymerase (Invitrogen Life Technologies). The full-length encoding sequence of mouse IFN-λ (GenBank, NM_001024673) was amplified from bone marrow cell-derived cDNA of BALB/c mice using the following primers: (forward) 5′-ATG CTC CTC CTG CTG TTG CCT CT-3′ and (reverse) 5′-TCA GAC ACA CTG GTC TCC A-3′. The PCR product was then inserted into the Zero Blunt TOPO PCR Cloning vector (pCR-Blunt II; Invitrogen Life Technologies). Following confirmation of the nucleotide sequence, the PCR product was inserted into the *Eco*RI site of the pCAGGS (28) or pcDNA3.1 vector (Invitrogen Life Technologies) to generate pCAGGS-mIFN-λ and pcDNA3.1-mIFN-λ, respectively. For the N-terminal FLAG-tagged versions (pCAGGS-FLAG-mIFN-λ and pcDNA3.1-FLAG-mIFN-λ), 5′-ACC ATG GAC TAC AAA GAC GAT GAC GAC AAG CTC CTC CTG CTG TTG CCT CTG-3′ were used as the forward primer. For the enrichment of transfected cells, the *Eco*RI fragment from pCR-Blunt II-mIFN-λ was inserted into pMACS K^K.II (Miltenyi Biotec) and pIRES2-enhanced GFP (EGFP) bicitronic vector (BD Biosciences) to generate pMACS K^K.II-mIFN-λ and pIRES2-mIFN-λ-EGFP, respectively. The expression plasmids for mouse IL-12 and IL-18, pCAGGS-IL-12, and pcDNA-mproIL-18-mICE have been described previously (19).

For receptor expression, the following primers were used: mCRF2–4 (mIL-28R) sense, 5′-GAA CAG GAG AGT GGA GTG AA-3′; mCRF2–4 (mIL-28R) antisense, 5′-GAC TCT TCG CTG ATG ATG CT-3′; mCRF2–12 (mIL-10Rβ) sense, 5′-ATG TGG CGG GCC GAC CGG TGG-3′; mCRF2–12 (mIL-10Rβ) antisense, 5′-CCT GCC GTG TGC GGA AGC TGC-3′; GAPDH sense, 5′-GTA TCG TGG AAG GAC TCA TG-3′; and GAPDH antisense, 5′-AGT GGG TGT CGC GCT GTT GAA G-3′. PCR conditions for each set of primers included initial treatment at 94°C for 2 min, followed by 35 cycles consisting of denaturation at 94°C for 15 s, annealing at 57°C for 30 s, followed by extension at 68°C for 2 min. PCR products were analyzed on a 1% agarose gel.

Transfection, colony formation assay, Western blotting, and caspase-3/7 assay

Cells (5×10^5) were transfected with plasmid DNA (1~8 μg) using Lipofectamine 2000 (Invitrogen Life Technologies). For the colony formation assay, cells were grown in regular medium for 2 days, followed by medium containing G418 geneticine (Invitrogen Life Technologies; 800 μg/ml) for 14 days. G418-resistant colonies >3 mm in diameter were counted. For Western blotting, cells were lysed by sonication in radioimmunoprecipitation assay buffer (29) and then centrifuged for 10 min at 4°C. Each cell extract (10 μg of protein) was assayed using the appropriate Abs and protein G-conjugated HRP (Amersham Biosciences). To detect caspase-3/7 activity, B16/F0 cells (1×10^6/60-mm plate) were transfected with pCAGGS-FLAG-IFN-λ (8 μg) or pCAGGS empty plasmid (8 μg), and cells (2×10^4/well of a 96-well plate) were plated 16 h following transfection. The Caspase-Glo 3/7 Assay system (Promega) was used according to the manufacturer's instructions 36 h after transfection. The background luminescence associated with cell culture and assay reagent (blank reaction) was subtracted from experimental values. Z-VAD-fmk (Promega) was used at 1 μM as an inhibitor of IFN-λ-mediated cell death. Means of triplicates were used to represent caspase-3/7 activity for the given cells. Each experiment was performed three times, with similar results.

Establishment of luciferase-expressing cells

Firefly (*Photinus pyralis*) luciferase cDNA from pGL3 basic (Promega) was inserted into the pMSCVpuro retroviral vector (Clonetech), generating pMSCV-luciferase. GP2-293 packaging cells (Clontech) were cotransfected with pMSCV-luciferase and pVSV-G (Clontech), a plasmid encoding the viral envelope glycoprotein (VSV-G) of the vesicular stomatitis virus, using Lipofectamine 2000 (Invitrogen Life Technologies). Supernatants from transfected GP2-293 were incubated with ~50% confluent B16/F10 and Colon26 cells in the presence of Polybrene (8 μg/ml final concentration; Sigma-Aldrich). Transduced cells were propagated in medium containing puromycin (Sigma-Aldrich) at 15 μg/ml (luc-B16/F10 and luc-Colon26).

Flow cytometry and magnetic bead selection

Cells (1×10^6) were washed with PBS and incubated with mAb for 30 min at 4°C. Following washing with 0.1% FCS-PBS, cells were analyzed using FACSCalibur (BD Biosciences) and FlowJo analysis software (Tree Star). For magnetic bead selection, pMACS K^K.II-mIFN-λ transfected B16 cells (5×10^6) were treated with MACSelect K^K MicroBeads (Miltenyi Biotec), washed, and then loaded onto a MACS MS column (Miltenyi Biotec) for positive magnet-based selection. Anti-NK Cell (DX5) MicroBeads were used for NK cell enrichment (the NK Isolation Kit; Miltenyi Biotec). The positive fraction was then analyzed by Western blotting and flow cytometry.

s.c. and i.v. tumor inoculation

Cells in exponential growth phase were harvested by trypsinization and washed twice in PBS before injection. For the s.c. injections, cells (1×10^6) were injected into the abdominal s.c. space of mice. Tumor growth at the skin was monitored by measurement of the two maximum perpendicular tumor diameters. For immunization, mice were injected twice (day 0 and 6) s.c. with 1×10^5 gamma-irradiated (80 Gy) cells that had been transiently transfected with plasmid DNA (2 μg). On day 12, spleen cells were harvested for CTL activity. For the i.v. injections to the lungs, luc-B16/F10 cells (5×10^4 in 0.2 ml of PBS) were injected into the tail vein of C57BL/6 mice. For tumor implantation to the liver, a midline incision was made on anesthetized mice, and 2×10^5 luc-Colon26 cells in 0.2 ml of PBS was injected into the ileocolic vein of BALB/c mice. Each experiment was performed two to four times, with similar results.

In vivo bioluminescence imaging

In vivo tumor progression was examined using the noninvasive bioimaging system IVIS (Xenogen). Tumor-implanted mice were anesthetized with a mixture of ketamine and xylazine, and D-luciferin (potassium salt; Biosynth) was injected into the peritoneal cavity at 2 mg/body, immediately followed by measurement of the luciferase activity. EnduRen (0.5–1.0 mg/body; Promega) was used to visualize *Renilla* (*Renilla reniformis*) luciferase expression from the pRL-TK vector (Promega). The imaging system consisted of a cooled, back-thinned charge-coupled device camera to capture both a visible light photograph of the animal taken with light emitting diodes and the luminescent image. After acquiring photographic images of each mouse, luminescent images were acquired with a 1- to 15-min exposure time (25, 26). Images were obtained with a 25-cm field of view, a binning (resolution) factor of 8, 1/f stop, and an open filter. The resulting gray scale photographic and pseudocolor luminescent images were automatically superimposed by software to facilitate identification and location of any optical signal on the mouse. Optical images were displayed and analyzed using Igor (WaveMetrics) and IVIS Living Image (Xenoxgen) software packages. The signal from tumors was quantified as photons flux in units of photons/sec/cm^2/steradian.

In vivo depletion of immune cells

Depleting anti-CD4 (clone GK1.5, rat IgG2b) and anti-CD8 (clone 2.43, rat IgG2b) mAbs were purified from the supernatant of hybridoma cells by passage through an affinity gel protein-G column (Amersham). To deplete host $CD4^+$ or $CD8^+$ T cells in vivo, animals received i.p. injection with purified mAbs (4 mg/kg) on days −1, 2, 5, 8, 12, and 14 of tumor inoculation. Anti-asialo GM1 Ab (100 μg/body; WAKO) was used to deplete NK cells. Control rat IgG was purchased from Sigma-Aldrich.

Histological examination

Removed specimens were fixed with 10% paraformaldehyde and embedded in paraffin. Sections were stained with H&E.

Hydrodynamic injection of plasmid DNA

Twenty micrograms of pCAGGS-FLAG-IFN-λ and 20 μg of pRL-TK were diluted in 1.6 ml of PBS (6.25% of body weight) (25) and injected into the tail or penile vein of BALB/c mice. The injection took no longer than 10 s, and the apnea period in mice ranged from 4 to 6 s. The *Renilla* luciferase-expressing pRL-TK vector was used to confirm liver targeting 24 h following hydrodynamic injection, and photons from *Renilla* luciferase were confirmed by IVIS (Xenogen).

Statistical analysis

Values of p were based on two-sided Student's t or Mann-Whitney U tests using the program Instat (GraphPad) for statistical evaluation. Differences between groups were considered significant if $p < 0.05$.

Results

Construction of the mouse IFN-λ expression vector and receptor expression in murine tumor cell lines

COS7 cells were transiently transduced with FLAG-tagged mouse IFN-λ cDNA and then subjected to Western blot analysis to examine the functional expression of cloned mouse IFN-λ (Fig. 1*a*). A 23-kDa protein was identified by the anti-FLAG-M2 mAb in a transfection-dependent manner. Furthermore, mouse IFN-λ and EGFP were coexpressed in B16/F10 cells by a bicistronic expression vector, and MHC class I expression (H-2K^b) was analyzed using flow cytometry after gating the EGFP-positive population (Fig. 1*b*). MHC class I expression was strongly enhanced following IFN-λ transduction but not by the mock transfection, and suggested that the transduced IFN-λ was functional. Interestingly, as with the case of IFN-α (6, 7), IFN-λ was able to induce cell surface expression of Fas in B16 cells (Fig. 1*d*).

The expression of IFN-λ receptor in murine tumor cell lines was also examined by RT-PCR (Fig. 1*e*). Although IL-10Rβ was expressed in all cell lines examined, IFN-λR (IL-28R) was expressed at various levels. B16 melanoma and Colon26 colon cancer cells expressed IFN-λR at higher levels. Thus, these cells could be potential targets of IFN-λ.

Overproduction of IFN-λ suppresses cell growth in vitro

B16/F0 and Colon26 cells were transduced with IFN-λ cDNA, and the generated G418-resistant cells were examined to determine the effect of IFN-λ on tumor growth. Immunoblot analysis did not show FLAG-tagged IFN-λ expression in cells derived from independent G418-resistant colonies (data not shown). The number of G418-resistant colonies following transfection was also evaluated (Fig. 2*a*). Colony formation (>3 mm in diameter) was significantly inhibited by IFN-λ cDNA and its FLAG-tagged version in comparison to the mock transfection (Fig. 2, *b* and *c*). Transient transfection of IFN-λ also induced retardation of cell growth in B16/F0 cells (Fig. 3*a*). Furthermore, we investigated whether overexpression of IFN-λ induced apoptotic cell death (Fig. 3*b*). IFN-λ-transduced B16/F0 cells showed significantly increased caspase-3/7 activity 36 h following transfection compared with the mock transduction, and a general caspase inhibitor (Z-VAD-fmk) effectively blocked IFN-λ-mediated apoptosis, demonstrating the specificity of the assay. Concomitant with increased caspase-3/7 activity, cell cycle regulator p21$^{Waf1/Cip1}$ induction and dephosphorylation of Rb (Ser^{780}) were also observed using Western blot analysis (Fig. 3*c*). Thus, these results demonstrated that overexpression of IFN-λ induces cell cycle arrest and apoptotic cell death in target tumor cells.

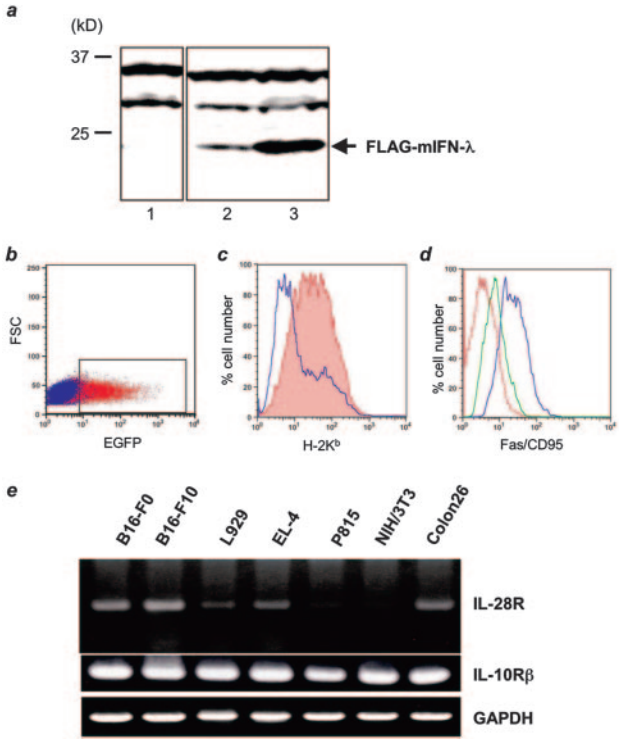

FIGURE 1. Functional expression of mouse IFN-λ and receptor expression in murine tumor cell lines. *a*, Following transient transduction of FLAG-tagged IFN-λ cDNA into COS7 cells, IFN-λ was detected by Western blotting using anti-FLAG M2 mAb. A single ~23-kDa band was detected in a dose- and transfection-dependent manner (*lane 1*, pCAGGS 8 μg; *lane 2*, pCAGGS-FLAG-mIFN-λ 4 μg; *lane 3*, pCAGGS-FLAG-mIFN-λ 8 μg). *b*, Mouse IFN-λ and EGFP were coexpressed in B16/F0 cells, and EGFP-positive cells were analyzed by flow cytometry (~40% was EGFP positive: red dots). Blue dots represent untransfected control cells. FSC, Forward scatter. *c*, In B16/F0 cells where IFN-λ and EGFP were coexpressed, MHC class I expression (H-2K^b) was analyzed after gating the EGFP-positive population. Red line, transfection of pIRE2-mIFN-λ-EGFP; blue line, transfection of pIRE2-EGFP alone. *d*, Fas expression in IFN-λ-expressed B16/F0 cells (blue line, stained with PE-conjugated anti-Fas mAb; red line, isotype-matched control). Green line represents mock-transfected B16/F0 cells stained with PE-conjugated anti-Fas mAb. *e*, IFN-λ receptor expression analysis in murine tumor cell lines using RT-PCR. *Upper panel*, IFN-λ receptor (IL-28R); *middle panel*, IL-10R β-chain; *lower panel*, GAPDH as an internal control.

Local expression of IFN-λ inhibits cutaneous tumor formation and pulmonary metastasis

In an effort to determine whether IFN-λ can inhibit in vivo tumor growth, Colon26 cells were transfected with IFN-λ cDNA and subsequently transplanted into the s.c. space of BALB/c mice. As shown in Fig. 4*a*, IFN-λ-transfected cells showed significantly retarded tumor growth compared with the mock transfection. Similar results were obtained in B16/F0 cells following IFN-λ cDNA treatment (data not shown).

We then investigated whether IFN-λ could prevent metastatic tumor growth. Luciferase-based luminescent imaging allowed us to quantitatively analyze the cellular process in living cells. Luciferase-expressing B16/F10 (luc-B16/F10) cells were used to visualize the fate of tumor progression in vivo (see *Materials and Methods*). The advantages of using luciferase as a marker include its sensitivity (as few as 50 luc-B16/F10 cells could be detected over background in vitro) and its linear dose-dependent output of light in the presence of D-luciferin (data not shown). Luc-B16/F10 cells were transiently transfected with

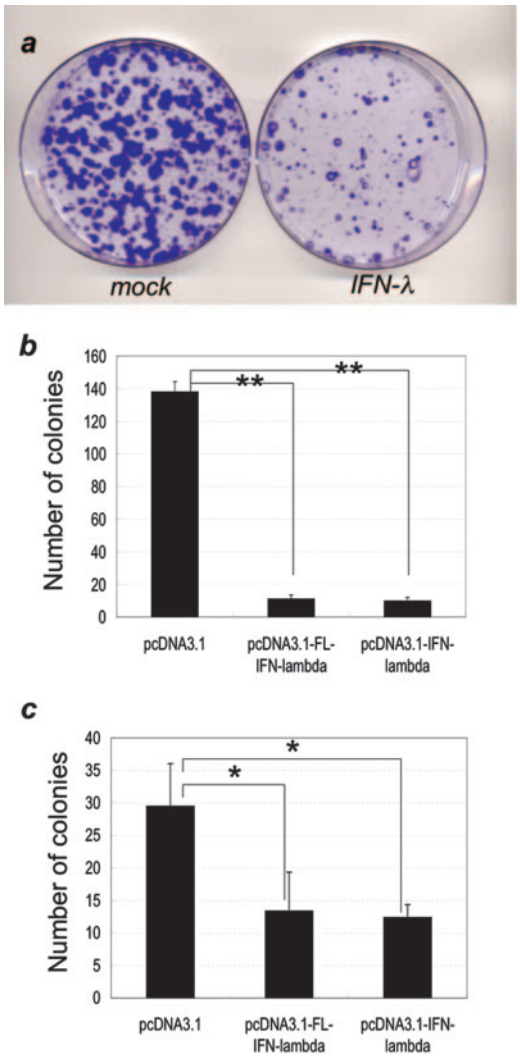

FIGURE 2. Mouse IFN-λ overproduction inhibits colony formation in vitro. *a*, Colony formation assay. B16/F0 cells were transduced with pcDNA3.1-mIFN-λ, and G418-resistant colonies were stained with methylene blue 14 days following transfection. *b*, B16/F0 and Colon26 cells (*c*) were transduced with pcDNA3.1-mIFN-λ, and G418-resistant colonies were counted 14 days following transfection. *, $p < 0.05$; **, $p < 0.01$ (Student's *t* test). One of two to three independent experiments with similar results is shown.

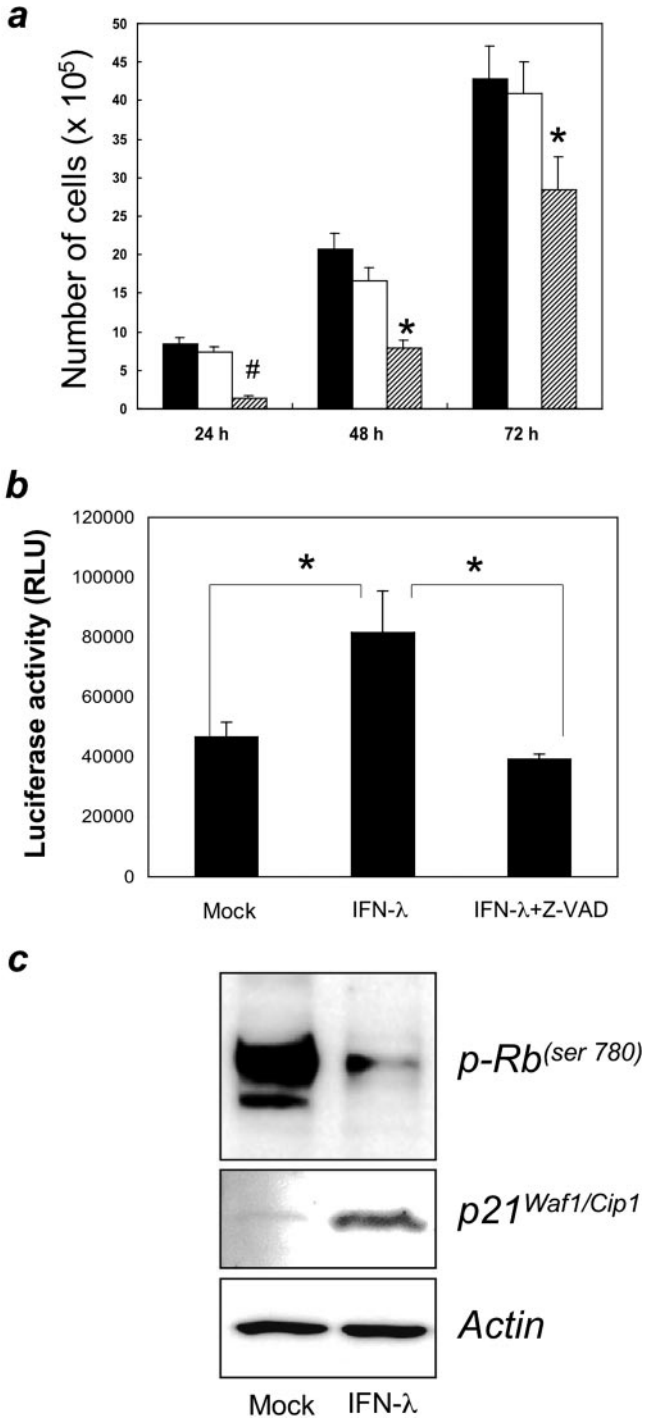

FIGURE 3. Effect of mouse IFN-λ overproduction on tumor cell growth in vitro. *a*, Cell growth retardation by IFN-λ expression. Following transient transfection of B16/F0 with pcDNA3.1-IFN-λ, cells (2×10^4/well in triplicate) were plated in vitro and then counted at the indicated time points. *b*, Caspase-3/7 activity was quantified 36 h following transient transfection of IFN-λ (see *Materials and Methods*). *, $p < 0.05$ (Student's *t* test). *c*, Cells (2×10^6) were transduced with pMACS-K^K.II-IFN-λ, and H-$2K^K$-positive cells were enriched by positive selection using magnetic bead isolation (~50% was H-$2K^K$-positive). Cells were lysed and analyzed for phospho-Rb (Ser^{780}), $p21^{Waf1/Cip1}$, and actin (as an internal control) by Western blotting.

IFN-λ and then injected into the tail vein of C57BL/6 mice. Pulmonary metastasis of luc-B16/F10 cells was monitored (Fig. 4, *b–d*). Strikingly, IFN-λ treatment prevented pulmonary metastasis 14 days following tumor injection (Fig. 4, *d–f*). Interestingly, histological examination of the lungs showed that IFN-λ treatment increased massive cellular infiltrates (Fig. 4, *g* and *h*), and suggested that immunological tumor destruction was also stimulated following IFN-λ treatment.

Implication of immune cells in IFN-λ-mediated tumor suppression

In an effort to determine whether $CD4^+$, $CD8^+$ T, or NK cells were involved in IFN-λ-mediated tumor destruction, anti-$CD4^+$, anti-$CD8^+$, and anti-asialo GM1 Abs were i.p. injected before s.c. tumor challenge of B16/F10 cells. As shown in Fig. 5, the in vivo depletion of NK cells facilitated progressive tumor growth following IFN-λ treatment compared with the control treatment ($p <$ 0.05). However, there was no difference in tumor growth in the $CD4^+$ and $CD8^+$ T cell-depleted group. Thus, these results suggested that NK cells are the predominant cells involved in the

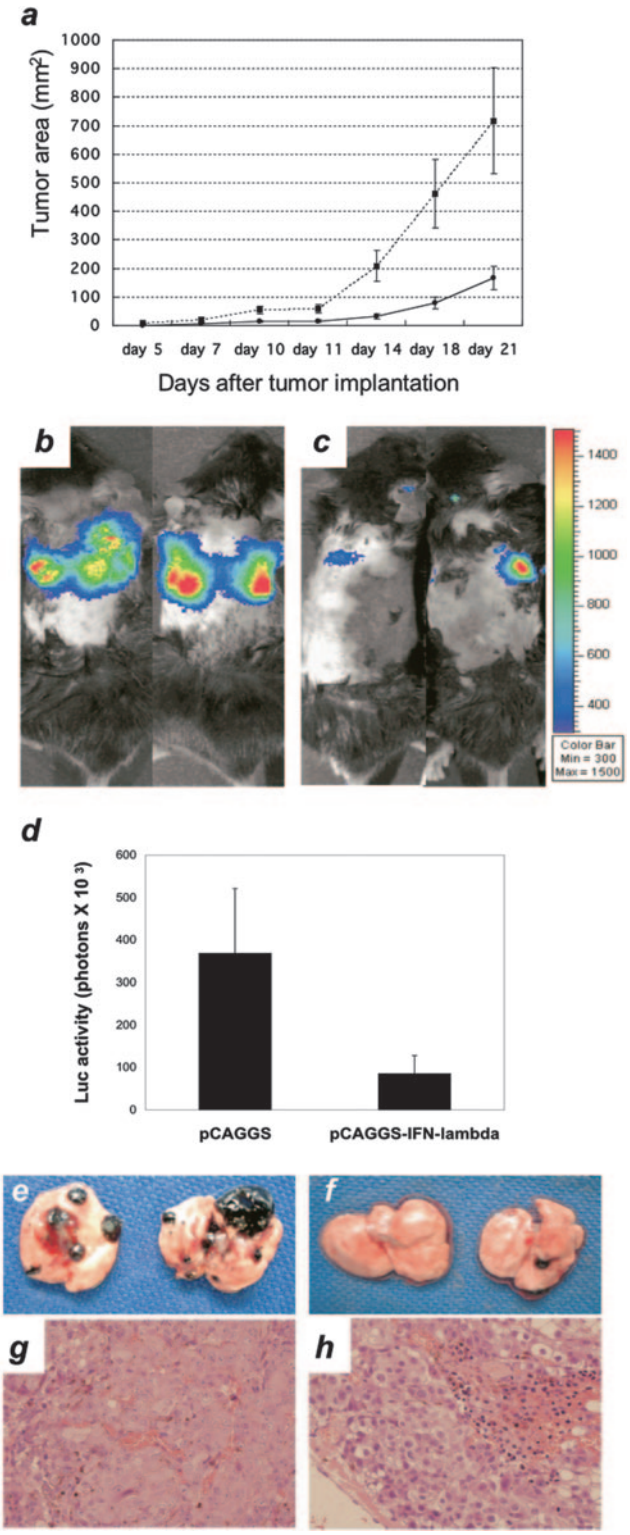

FIGURE 4. IFN-λ expression inhibits primary and metastatic tumor growth. *a*, Colon26 cells transiently expressing IFN-λ were transplanted into the s.c. space of BALB/c mice, and tumor growth was measured at the indicated time points. *b* and *c*, In vivo luminescent imaging based on the presence of luciferase in tumor cells demonstrated decreased pulmonary metastasis of IFN-λ-overexpressing luc-B16/F10 cells (*c*) compared with the mock transfection (*b*). *d*, Pulmonary metastasis was evaluated by tumor-derived photon counting using an in vivo luminescent imaging system. Visual (*e* and *f*) and histological (*g* and *h*) examination of the same lungs demonstrated decreased metastatic growth in IFN-λ-overexpressing B16/F10 cells (*f* and *h*), but not in mock-transfected cells (*e* and *g*) at 14 days following tumor injection (H&E, original magnification ×100).

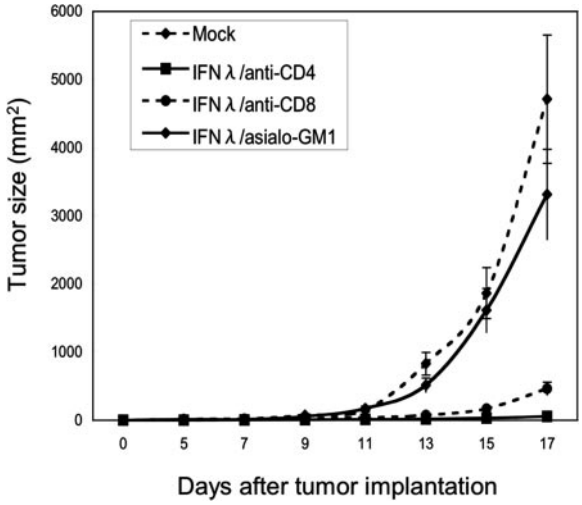

FIGURE 5. Effect of anti-CD4, anti-CD8, and anti-asialo GM1 Abs on IFN-λ-mediated tumor suppression. In vivo immune cell depletion with anti-asialo GM1 Abs resulted in significant suppression of the antitumor effect of IFN-λ-overexpression ($p < 0.05$, vs anti-CD4 and anti-CD8). The error bars represent the mean ± SD ($n = 5–6$).

antitumor effect of IFN-λ, and that $CD4^+$ and $CD8^+$ T cells contribute less to IFN-λ-induced tumor destruction.

Targeting of liver metastatic foci by hydrodynamic delivery of IFN-λ expression plasmid

Several studies, including those of our own group, have shown that systemic injection through the vein using a large volume of plasmid DNA solution (hydrodynamic gene delivery) can achieve efficient gene transfer into the liver. We therefore examined whether hydrodynamic gene delivery of IFN-λ could inhibit liver metastatic growth of Colon26 cells. Luciferase-transduced Colon26 cells (5×10^5) were inoculated into the liver of BALB/c mice through the portal vein, and naked plasmid DNA of IFN-λ was injected i.v. into the penile vein of mice 3 days following posttumor inoculation. The therapeutic vector was coinjected with a pRL-TK *Renilla*-derived luciferase expression vector to monitor liver-selective gene delivery (Fig. 6*a*). Tumor formation in the liver was measured by in vivo luminescent imaging (Fig. 6*b*). Hydrodynamic injection of IFN-λ cDNA demonstrated significant retardation of tumor growth around day 9 posttumor injection compared with the mock plasmid injection. Tumor-derived photons with IFN-λ treatment were at a third of the level of the mock treatment at day 12 (Fig. 6*c*). Mice receiving IFN-λ cDNA possessed moderately better survival (Fig. 6*d*), and tumor-derived photons were not observed in 10–20% of mice undergoing IFN-λ-treatment on day 30. These mice were not free from the second tumor challenge at the s.c. site, but their tumor growth was retarded in comparison with that of naive mice, suggesting that IFN-λ may make a modest contribution to long-term antitumor immunity.

In an effort to address whether IFN-λ can support systemic CTL responses, tumor-killing activity was evaluated in vitro using spleen cells from C57BL/6 mice that were immunized by s.c. injection of irradiated IFN-λ-transduced B16/F10 cells (Fig. 6*e*). Because IL-12 and IL-18 efficiently introduce systemic CTLs (30–32), we used IL-12 and IL-18 expression plasmids as a control transduction. Spleen cells from immunized mice with IFN-λ treatment demonstrated efficient killing of B16/F10 cells in vitro, and results were equivalent to immunization using IL-12/IL-18-transduced B16/F10 cells. Immunization with mock transduction

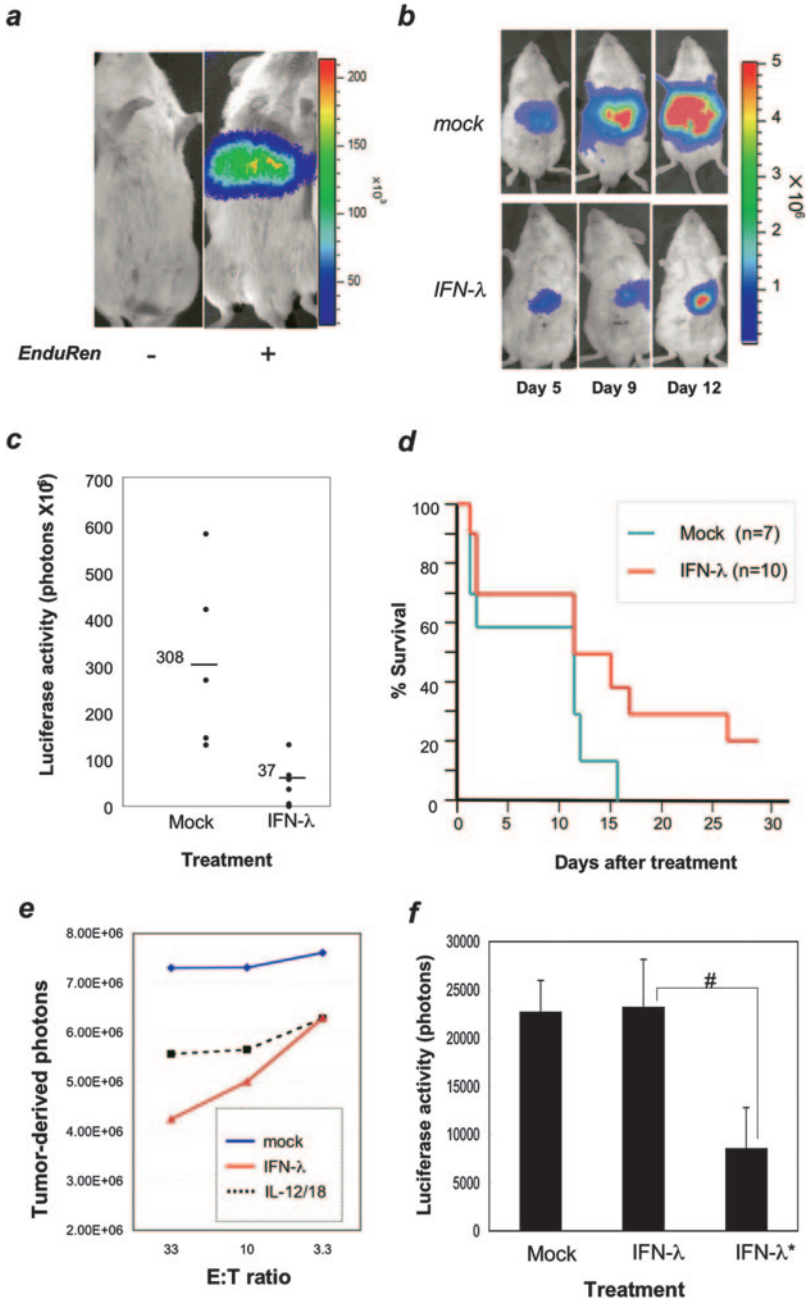

FIGURE 6. Targeting therapy of liver metastasis by hydrodynamic injection of IFN-λ cDNA. Luc-Colon26 cells were implanted into the liver through the portal vein of BALB/c mice (*a–d*). *a*, *Renilla* luciferase expression plasmid pRL-TK was used as a coinjection marker for the hydrodynamic therapeutic procedure. Substantial photons were obtained specifically from the liver of BALB/c mice in the presence of EnduRen (Promega). *b*, Representative firefly luciferase imaging of tumor-burdened animals following mock (*upper panels*) or IFN-λ (*lower panels*) treatment at the indicated time points. *c*, Liver metastasis of luc-Colon26 cells was evaluated by photon counting ($p = 0.0031$, Mann-Whitney *U* test). *d*, IFN-λ improves the survival rate in liver-metastasized mice ($p = 0.04$, log-rank test). *e*, Cytotoxic assay against luc-B16/F10 cells. C57BL/6J mice were immunized by s.c. injection of irradiated cDNA-transduced B16/F10 cells. Spleen cells from immunized mice were used as effectors at the indicated E:T ratios. Photons represent cell viability from luc-B16/F10 cells 12 h following incubation with effector lymphocytes. Data are shown as the average of triplicate assays. Mock, pCAGGS; IFN-λ, pCAGGS-mIFN-λ; IL-12/18, pCAGGS-IL-12 plus pcDNA-mproIL-18-mICE. *f*, Luc-B16/F10 cells were implanted into the lungs through the tail vein of C57BL/6J mice. Pulmonary metastasis of luc-B16/F10 cells was evaluated by tumor-derived photon counting following hydrodynamic gene delivery (day 15 after tumor implantation). #, $p = 0.018$ vs ∗IFN-λ. ∗, Transiently IFN-λ-expressing luc-B16/F10 cells implanted without hydrodynamic gene delivery.

was unable to induce sufficient tumor-killing activity. Thus, these results demonstrate that active immunization using IFN-λ can support systemic CTL-inducing activity.

Furthermore, we examined whether pulmonary metastasis of luc-B16/F10 cells could be inhibited by hydrodynamic delivery of IFN-λ cDNA (Fig. 6*f*). Tumor-derived photons in the lungs could not be segregated between control and IFN-λ cDNA injections at day 15 after tumor implantation ($p = 0.7$). However, IFN-λ-transduced luc-B16/F10 cells significantly suppressed the metastatic growth ($p < 0.05$). These results therefore demonstrate that local delivery of IFN-λ is necessary for the control of metastatic tumor growth at target sites, and suggest that the IFN-λ-meditated systemic CTL response is only weak.

IFN-λ increased the number of NK and NKT cells in the liver of mice

To address the role of IFN-λ expression in the liver, hepatic lymphocytes were isolated following hydrodynamic injection of IFN-λ cDNA and analyzed by flow cytometry. As shown in Fig. 7*a*, the number of NK and NKT cells increased compared with the mock injection 2 days following IFN-λ cDNA injection: $CD3^-NK1.1^+$ cells increased from 10.9 to 26.9%, whereas $CD3^+NK1.1^+$ cells increased from 1.0 to 11.0%. There was no significant increase in the total number of hepatic lymphocytes. Furthermore, IFN-λ-exposed liver lymphocytes displayed significant killing activity against luc-Colon26 cells (Fig. 7*b*). In fact, $CD3^-DX5^+$ cells substantially expressed IFN-λR and IL-10Rβ (Fig. 7*c*), and their IFN-λ-exposure moderately enhanced killing of luc-Colon26 cells (Fig. 7*d*). The NK cell depletion in vivo using anti-asialo GM1 Abs also demonstrates that functional NK cell activity against the luc-Colon26 tumor was elicited following IFN-λ cDNA treatment (Fig. 7, *d* and *e*). These results therefore demonstrated that forced expression of IFN-λ in the liver enhances the number of NK and NKT cells and augments their killing activity against tumors. This suggested that IFN-λ stimulates the innate immune system and may lead to the antitumor immunity.

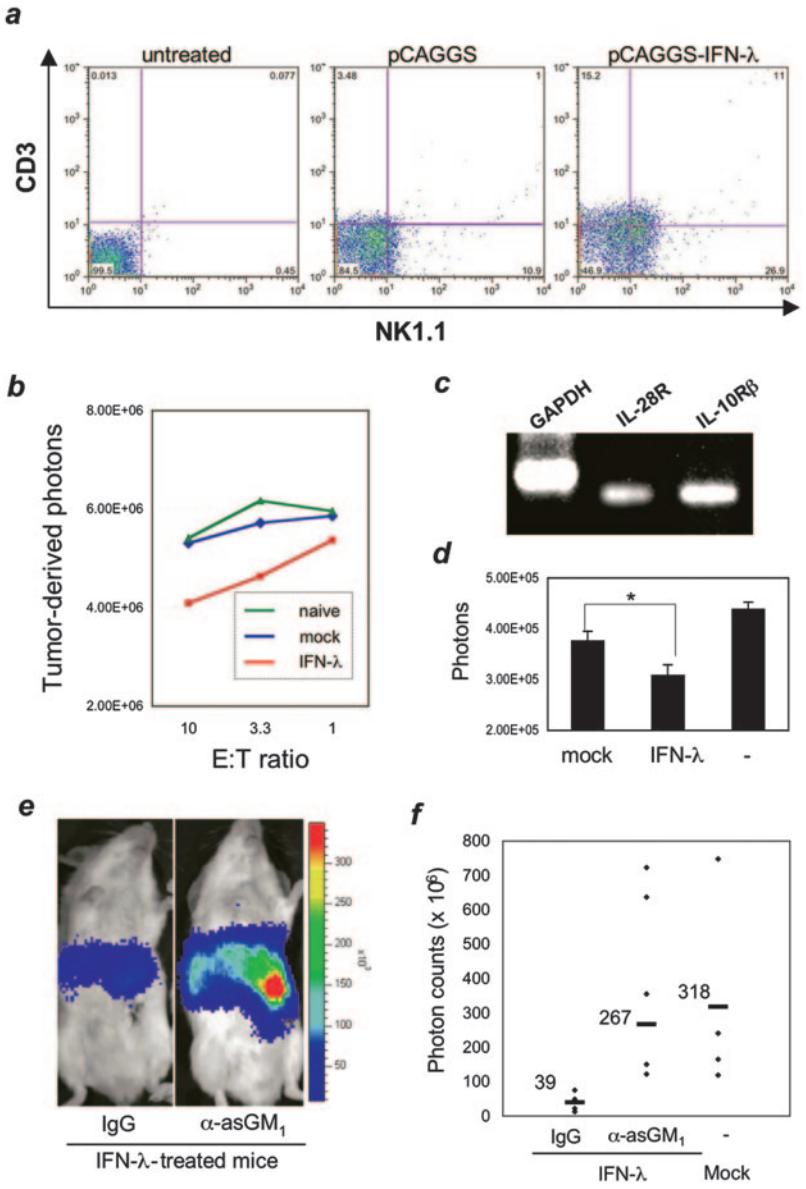

FIGURE 7. Flow cytometric analysis of intrahepatic lymphocytes. The liver of mice that underwent hydrodynamic injection was perfused with 0.1%-EDTA-PBS, and liver lymphocytes were isolated by Ficoll gradient centrifugation at 400 × *g* for 20 min. *a*, The isolated hepatic lymphocytes were stained using FITC-conjugated anti-mouse CD3ε (145-2C11) and PE-conjugated anti-mouse NK1.1 (PK136) mAbs, and then analyzed using flow cytometry. Data represent one of two independent experiments with similar results. *b*, Cytotoxic assay against luc-Colon26 cells. Intrahepatic lymphocytes were used as effectors at the indicated E:T ratios. Photons represent cell viability from luc-Colon26 cells 12 h following incubation with hepatic lymphocytes. Data are shown as the average of triplicate assays (one of three independent experiments with similar results). *c*, IFN-λ receptor expression in $CD3^{-}DX5^{+}$ NK cells using RT-PCR. FACS analysis showed enrichment to >90% homogeneity. *d*, Cytotoxicity against luc-Colon26 cells using $DX5^{+}$ NK cells. $DX5^{+}$ NK cells were used as effectors at an E:T ratio of 20. Data are shown as the average of triplicate assays (one of two independent experiments with similar results). ∗, $p = 0.03$ (Student's *t* test). *e* and *f*, In vivo NK cell depletion with anti-asialo GM1 Abs abrogates IFN-λ-mediated tumor eradication in the liver. *e*, Representative luciferase imaging of luc-Colon26 liver tumor in the presence of control (IgG) or anti-asialo GM1 (α-asGM1) Abs following IFN-λ cDNA treatment. *f*, Liver metastasis of luc-Colon26 cells was evaluated by photon counting at day 9 posttumor implantation (α-asGM1 vs IgG; $p = 0.016$, Mann-Whitney *U* test). One of two independent experiments with similar results.

Discussion

We demonstrated the antitumor effect of mouse IFN-λ against murine tumor cells. The remarkable features presented in this study include the following: 1) IFN-λ induced cell cycle arrest and apoptotic cell death in vitro; 2) overexpression of IFN-λ inhibited s.c. and metastatic tumor formation in vivo; 3) NK cells were critical to IFN-λ-mediated tumor growth inhibition in vivo; and 4) hydrodynamic delivery of IFN-λ cDNA achieved effective tumor targeting in liver metastatic foci.

Type I IFNs have been used for multiple clinical indications including malignant diseases, multiple sclerosis, and chronic hepatitis B and C (12). Because human IL-28 and IL-29 can be induced following viral infection (14–17) and treatment with IFN-α (33), their forced expression needed to be evaluated in terms of their antitumor activity (Figs. 2–4). Although Dumoutier et al. (16) showed an anti-proliferative effect of IFN-λ in lymphoma cells, they did not demonstrate any substantial apoptotic effects. Melanoma B16 cells are less immunogenic and highly resistant to a variety of apoptotic stimuli such as anticancer agents if they are not manipulated (34–36). However, overexpression of IFN-λ in B16 cells induced cell surface MHC class I and Fas (CD95) and, moreover, markedly increased caspase-3/7 activity concomitant with cell cycle arrest (Fig. 3). These changes could provide T cells with an enhanced ability to recognize and destroy target tumor cells. Nonetheless, because expression of the IL-28R in tumor cell lines was limited, local overexpression or intracellular expression of IFN-λ and its engagement may require the transduction of a signal to induce apoptosis. Given the decreased affinity for the receptor (14) and varied activity of different signal-transducing molecules (16), the appropriate expression of the ligand therefore appears to yield a sufficient antitumor effect.

Substantial in vivo antitumor and antimetastatic activity was demonstrated by overproducing IFN-λ (Fig. 4). Type I IFNs possess immunoregulatory functions as well as antiviral and antitumor activity. For example, IFN-α promotes phenotypic differentiation and increases MHC class I expression in normal and tumor cells, and serves as a critical link between innate and adaptive immunity (6, 7, 33), in addition to being able to activate DCs, NK cells, and macrophages. In synergy with IL-18, IFN-α enhances IFN-γ production in NK and T cells (37, 38). IFN-γ in turn can facilitate Ag presentation in DCs and macrophages, resulting in activation of adaptive immunity and elimination of tumor and virus-infected

cells by CTLs. However, whereas active immunization using IFN-λ was able to induce CTLs (Fig. 6*e*), our animal experiments in vivo using gene transfer of IFN-λ demonstrated only a modest CTL response. Our Ab-mediated immunodepletion experiments showed that NK cells were the predominant cells involved in the in vivo antitumor activity of IFN-λ (Fig. 5). Regarding NK cell-mediated CTL induction, there is emerging data suggesting that induction of tumor-specific T cell memory is dependent upon NK cell-mediated tumor rejection (39, 40). Our data therefore suggest that resident NK cells at the site may be critical targets for IFN-λ, and that IFN-λ may serve as a transducer inducing the innate immune response to adaptive immunity. This indirect pathway may explain why the CTL response by gene transfer of IFN-λ was still modest.

Furthermore, type I IFNs can reduce the amount of angiogenic growth factors in many tumor cells such as basic fibroblast growth factor (41, 42), inhibiting tumor formation. Because the observed IFN-λ response was similar to the signal transduction pathway observed for type I IFNs (16), IFN-λ might possess potent anti-angiogenic activity against tumor growth in vivo.

The intravascular delivery of naked plasmid DNA through the vein is an effective method for transferring DNA into the rodent liver. Systemic injection through a tail vein with a large volume of plasmid DNA solution can achieve effective gene transfer into the liver (23, 24). This liver-targeted strategy possesses the following advantages: 1) the liver is the largest organ of the reticuloendothelial system and appropriate immunological responses could be introduced; and 2) plasmid DNA can potentially activate the TLR 9 that mediates innate immune reactions (43, 44). The liver contains >70% of all tissue macrophages (Kupffer cells) and eliminates bacteria and foreign bodies from the circulation. The liver can respond rapidly to proinflammatory cytokines including IL-1β and TNF-α, and hepatic sinusoidal lymphocytes also exert effects on NK cells (45). Numerous studies in recent years have examined the potential of using DNA containing the CpG-motif, alone and in combination with other molecules, to boost the immunological response in a variety of disease settings including the treatment of cancer (46, 47). Furthermore, DNA containing the CpG-motif can stimulate many DCs, leading to increased expression of MHC and costimulatory molecules, and the production of proinflammatory cytokines (48, 49). With regard to liver targeting, our previous studies using a particle-mediated gene transfer method also demonstrated that primary hepatic immunization gave rise to a beneficial immune response against malaria, in which cellular and humoral immune responses were induced (21, 50, 51). Thus, hepatic gene delivery of IFN-λ that activates NK/NKT cells could be useful in immunotherapy and may represent a reasonable approach for the management of liver metastasis.

Although hydrodynamic injection is a powerful gene delivery system for rodent animals, there are obvious clinical limitations associated with this method that relate to injection volume and rate. Volume and rate of injection are critical in the uptake of naked DNA plasmids, because a large fluid volume is needed (i.e., equivalent of the animal's blood volume) and it must be injected rapidly (23). In fact, it has been reported that symptoms of transient cardiac failure are observed even in rodent animals during and immediately after injection (25). Thus, hydrodynamic gene delivery cannot be translated to clinical settings until the adverse effects of this procedure are overcome.

The therapeutic options for patients with metastatic disease remain limited, and the majority of these patients will subsequently develop a local or systemic recurrence following the local treatment of liver metastases (52, 53). A new treatment modality to control local disease and prevent systemic progression is required. Interestingly, whereas 57% of mice with tumors subjected to hydrodynamic therapy with mouse IFN-α cDNA died within 24 h, only 13% of IFN-λ cDNA-treated mice died 24 h following treatment (data not shown). These data reflect the lower toxicity of IFN-λ. Overall, local immunotherapy still remains an attractive approach to control liver metastasis, and use of IFN-λ might prove a useful adjunctive strategy in the clinical treatment of human malignancies. Nonetheless, it remains of utmost importance to carefully examine the clinical data for evidence to support or refute the notion that use of IFN-λ enhances the regulation of human malignancy.

Acknowledgments

We thank Yasuko Sakuma and Harumi Kawana for their skillful technical assistance.

Disclosures

The authors have no financial conflict of interest.

References

1. Rosenberg, S. A., J. C. Yang, and N. P. Restifo. 2004. Cancer immunotherapy: moving beyond current vaccines. *Nat. Med.* 10: 909–915.
2. Li, Y., and E. F. McClay. 2002. Systemic chemotherapy for the treatment of metastatic melanoma. *Semin. Oncol.* 29: 413–426.
3. Vaishampayan, U., J. Abrams, D. Darrah, V. Jones, and M.S. Mitchell. 2002. Active immunotherapy of metastatic melanoma with allogeneic melanoma lysates and interferon α. *Clin. Cancer Res.* 8: 3696–3701.
4. Tsao, H., M. B. Atkins, and A. J. Sober. 2004. Management of cutaneous melanoma. *N. Engl. J. Med.* 351: 998–1012.
5. Murphy, A., J. A. Westwood, M. W. Teng, M. Moeller, P. K. Darcy, and M. H. Kershaw. 2005. Gene modification strategies to induce tumor immunity. *Immunity* 22: 403–414.
6. Biron, C. A. 2001. Interferons α and β as immune regulators: a new look. *Immunity* 14: 661–664.
7. Le Bon, A., and D. F. Tough. 2002. Links between innate and adaptive immunity via type I interferon. *Curr. Opin. Immunol.* 14: 432–436.
8. Langer, J. A., E. C. Cutrone, and S. Kotenko. 2004. The class II cytokine receptor (CRF2) family: overview and patterns of receptor-ligand interactions. *Cytokine Growth Factor Rev.* 15: 33–48.
9. Fellous, M., U. Nir, D. Wallach, G. Merlin, M. Rubinstein, and M. Revel. 1982. Interferon-dependent induction of mRNA for the major histocompatibility antigens in human fibroblasts and lymphoblastoid cells. *Proc. Natl. Acad. Sci. USA* 79: 3082–3086.
10. Marrack, P., J. Kappler, and T. Mitchell. 1999. Type I interferons keep activated T cells alive. *J. Exp. Med.* 189: 521–530.
11. Montoya, M., G. Schiavoni, F. Mattei, I. Gresser, F. Belardelli, P. Borrow, and D. F. Tough. 2002. Type I interferons produced by dendritic cells promote their phenotypic and functional activation. *Blood* 99: 3263–3271.
12. Gutterman, J. U. 1994. Cytokine therapeutics: lessons from interferon α. *Proc. Natl. Acad. Sci. USA* 91: 1198–1205.
13. Dusheiko, G. 1997. Side effects of α interferon in chronic hepatitis C. *Hepatology* 26(3 Suppl. 1): 112–121.
14. Sheppard, P., W. Kindsvogel, W. Xu, K. Henderson, S. Schlutsmeyer, T. E. Whitmore, R. Kuestner, U. Garrigues, C. Birks, J. Roraback, et al. 2003. IL-28, IL-29 and their class II cytokine receptor IL-28R. *Nat. Immunol.* 4: 63–68.
15. Kotenko, S. V., G. Gallagher, V. V. Baurin, A. Lewis-Antes, M. Shen, N. K. Shah, J. A. Langer, F. Sheikh, H. Dickensheets, and R. P. Donnelly. 2003. IFN-λs mediate antiviral protection through a distinct class II cytokine receptor complex. *Nat. Immunol.* 4: 69–77.
16. Dumoutier, L., A. Tounsi, T. Michiels, C. Sommereyns, S. V. Kotenko, and J. C. Renauld. 2004. Role of the interleukin (IL)-28 receptor tyrosine residues for antiviral and antiproliferative activity of IL-29/interferon-λ 1: similarities with type I interferon signaling. *J. Biol. Chem.* 279: 32269–32274.
17. Robek, M. D., B. S. Boy, and F. V. Chisari. 2005. λ Interferon inhibits hepatitis B and C virus replication. *J. Virol.* 79: 3851–3854.
18. Wang, J., T. Murakami, Y. Hakamata, T. Ajiki, Y. Jinbu, Y. Akasaka, M. Ohtsuki, H. Nakagawa, and E. Kobayashi. 2001. Gene gun-mediated oral mucosal transfer of interleukin 12 cDNA coupled with an irradiated melanoma vaccine in a hamster model: successful treatment of oral melanoma and distant skin lesion. *Cancer Gene Ther.* 8: 705–712.
19. Ajiki, T., T. Murakami, Y. Kobayashi, Y. Hakamata, J. Wang, S. Inoue, M. Ohtsuki, H. Nakagawa, Y. Kariya, Y. Hoshino, and E. Kobayashi. 2003. Long-lasting gene expression by particle-mediated intramuscular transfection modified with bupivacaine: combinatorial gene therapy with IL-12 and IL-18 cDNA against rat sarcoma at a distant site. *Cancer Gene Ther.* 10: 318–329.
20. Wang, J., T. Murakami, S. Yoshida, H. Matsuoka, A. Ishii, T. Tanaka, K. Tobita, M. Ohtsuki, H. Nakagawa, M. Kusama, and E. Kobayashi. 2003. Predominant cell-mediated immunity in the oral mucosa: gene gun-based vaccination against infectious diseases. *J. Dermatol. Sci.* 31: 203–210.

21. Nakamura, M., J. Wang, T. Murakami, T. Ajiki, Y. Hakamata, T. Kaneko, M. Takahashi, H. Okamoto, M. Mayumi, and E. Kobayashi. 2003. DNA immunization of the grafted liver by particle-mediated gene gun. *Transplantation* 76: 1369–1375.
22. Wang, J., Y. Kobayashi, A. Sato, E. Kobayashi, and Murakami, T. 2004. Synergistic anti-tumor effect by combinatorial gene-gun therapy using IL-23 and IL-18 cDNA. *J. Dermatol. Sci.* 36: 66–68.
23. Liu, F., Y. Song, and D. Liu. 1999. Hydrodynamics-based transfection in animals by systemic administration of plasmid DNA. *Gene Ther.* 6: 1258–1266.
24. Zhang, G., V. Budker, and J. A. Wolff. 1999. High levels of foreign gene expression in hepatocytes after tail vein injections of naked plasmid DNA. *Hum. Gene Ther.* 10: 1735–1737.
25. Inoue, S., Y. Hakamata, M. Kaneko, and E. Kobayashi. 2004. Gene therapy for organ grafts using rapid injection of naked DNA: application to the rat liver. *Transplantation* 77: 997–1003.
26. Sato, Y., T. Ajiki, S. Inoue, J. Fujishiro, H. Yoshino, Y. Igarashi, Y. Hakamata, T. Kaneko, T. Murakami, and E. Kobayashi. 2005. Gene silencing in rat-liver and limb grafts by rapid injection of small interference RNA. *Transplantation* 79: 240–243.
27. Murakami, T., W. Maki, A. R. Cardones, H. Fang, A. Tun Kyi, F. O. Nestle, and S. T. Hwang. 2002. Expression of CXC chemokine receptor-4 enhances the pulmonary metastatic potential of murine B16 melanoma cells. *Cancer Res.* 62: 7328–7334.
28. Niwa, H., K. Yamamura, and J. Miyazaki. 1991. Efficient selection for high-expression transfectants with a novel eukaryotic vector. *Gene* 108: 193–199.
29. Murakami, T., H. Hirai, T. Suzuki, J. Fujisawa, and M. Yoshida. 1995. HTLV-1 Tax enhances NF-κ B2 expression and binds to the products p52 and p100, but does not suppress the inhibitory function of p100. *Virology* 206: 1066–1074.
30. Neighbors, M., X. Xu, F. J. Barrat, S. R. Ruuls, T. Churakova, R. Debets, J. F. Bazan, R. A. Kastelein, J. S. Abrams, and A. O'Garra. 2001. A critical role for interleukin 18 in primary and memory effector responses to *Listeria monocytogenes* that extends beyond its effects on interferon γ production. *J. Exp. Med.* 194: 343–354.
31. Tough, D. F., X. Zhang, and J. Sprent. 2001. An IFN-γ-dependent pathway controls stimulation of memory phenotype $CD8^+$ T cell turnover in vivo by IL-12, IL-18, and IFN-γ. *J. Immunol.* 166: 6007–6011.
32. Raue, H. P., J. D. Brien, E. Hammarlund, and M. K. Slifka. 2004. Activation of virus-specific $CD8^+$ T cells by lipopolysaccharide-induced IL-12 and IL-18. *J. Immunol.* 173: 6873–6881.
33. Siren, J., J. Pirhonen, I. Julkunen, and S. Matikainen. 2005. IFN-α regulates TLR-dependent gene expression of IFN-α, IFN-β, IL-28, and IL-29. *J. Immunol.* 174: 1932–1937.
34. Ivanov, V. N., A. Bhoumik, and Z. Ronai. 2003. Death receptors and melanoma resistance to apoptosis. *Oncogene* 22: 3152–3161.
35. Murakami, T., A. R. Cardones, S. E. Finkelstein, N. P. Restifo, B. A. Klaunberg, F. O. Nestle, S. S. Castillo, P. A. Dennis, and S. T. Hwang. 2003. Immune evasion by murine melanoma mediated through CC chemokine receptor-10. *J. Exp. Med.* 198: 1337–1347.
36. Sredni, B., M. Weil, G. Khomenok, I. Lebenthal, S. Teitz, Y. Mardor, Z. Ram, A. Orenstein, A. Kershenovich, S. Michowiz, et al. 2004. Ammonium trichloro-(dioxoethylene-o,o')tellurate (AS101) sensitizes tumors to chemotherapy by inhibiting the tumor interleukin 10 autocrine loop. *Cancer Res.* 64: 1843–1852.
37. Matikainen, S., A. Paananen, M. Miettinen, M. Kurimoto, T. Timonen, I. Julkunen, and T. Sareneva. 2001. IFN-α and IL-18 synergistically enhance IFN-γ production in human NK cells: differential regulation of Stat4 activation and IFN-γ gene expression by IFN-α and IL-12. *Eur. J. Immunol.* 31: 2236–2245.
38. Sareneva, T., I. Julkunen, and S. Matikainen. 2000. IFN-α and IL-12 induce IL-18 receptor gene expression in human NK and T cells. *J. Immunol.* 165: 1933–1938.
39. Kelly, J. M., P. K. Darcy, J. L. Markby, D. I. Godfrey, K. Takeda, H. Yagita, and M. J. Smyth. 2002. Induction of tumor-specific T cell memory by NK cell-mediated tumor rejection. *Nat. Immunol.* 3: 83–90.
40. Raulet, D. H. 2004. Interplay of natural killer cells and their receptors with the adaptive immune response. *Nat. Immunol.* 5: 996–1002.
41. Singh, R. K., M. Gutman, C. D. Bucana, R. Sanchez, N. Llansa, I. J. Fidler. 1995. Interferons α and β down-regulate the expression of basic fibroblast growth factor in human carcinomas. *Proc. Natl. Acad. Sci. USA* 92: 4562–4566.
42. Fidler, I. J. 2001. Regulation of neoplastic angiogenesis. *J. Natl. Cancer Inst. Monogr.* 28: 10–14.
43. Hemmi, H., O. Takeuchi, T. Kawai, T. Kaisho, S. Sato, H. Sanjo, M. Matsumoto, K. Hoshino, H. Wagner, K. Takeda, and S. Akira. 2000. A Toll-like receptor recognizes bacterial DNA. *Nature* 408: 740–745.
44. Takeshita, F., C. A. Leifer, I. Gursel, K. J. Ishii, S. Takeshita, M. Gursel, and D. M. Klinman. 2001. Role of Toll-like receptor 9 in CpG DNA-induced activation of human cells. *J. Immunol.* 167: 3555–3558.
45. Malter, M., E. Friedrich, and R. Suss. 1986. Liver as a tumor cell killing organ: Kupffer cells and natural killers. *Cancer Res.* 46: 3055–3060.
46. Weiner, G. J., H. M. Liu, J. E. Wooldridge, C. E. Dahle, and A. M. Krieg. 1997. Immunostimulatory oligodeoxynucleotides containing the CpG motif are effective as immune adjuvants in tumor antigen immunization. *Proc. Natl. Acad. Sci. USA* 94: 10833–10837.
47. Krieg, A. M. 2002. CpG motifs in bacterial DNA and their immune effects. *Annu. Rev. Immunol.* 20: 709–760.
48. Krug, A., S. Rothenfusser, V. Hornung, B. Jahrsdorfer, S. Blackwell, Z. K. Ballas, S. Endres, A. M. Krieg, and G. Hartmann. 2001. Identification of CpG oligonucleotide sequences with high induction of IFN-αβ in plasmacytoid dendritic cells. *Eur. J. Immunol.* 31: 2154–2163.
49. Hartmann, E., B. Wollenberg, S. Rothenfusser, M. Wagner, D. Wellisch, B. Mack, T. Giese, O. Gires, S. Endres, and G. Hartmann. 2003. Identification and functional analysis of tumor-infiltrating plasmacytoid dendritic cells in head and neck cancer. *Cancer Res.* 63: 6478–6487.
50. Yoshida, S., S. I. Kashiwamura, Y. Hosoya, E. Luo, H. Matsuoka, A. Ishii, A. Fujimura, and E. Kobayashi. 2000. Direct immunization of malaria DNA vaccine into the liver by gene gun protects against lethal challenge of *Plasmodium berghei* sporozoite. *Biochem. Biophys. Res. Commun.* 271: 107–115.
51. Coban, C., K. J. Ishii, T. Kawai, H. Hemmi, S. Sato, S. Uematsu, M. Yamamoto, O. Takeuchi, S. Itagaki, N. Kumar, et al. 2005. Toll-like receptor 9 mediates innate immune activation by the malaria pigment hemozoin. *J. Exp. Med.* 201: 19–25.
52. Hohenberger, P., P. Schlag, V. Schwarz, and C. Herfarth. 1990. Tumor recurrence and options for further treatment after resection of liver metastases in patients with colorectal cancer. *J. Surg. Oncol.* 44: 245–251.
53. Sato, T. 2002. Locoregional immuno(bio)therapy for liver metastases. *Semin. Oncol.* 29: 160–167.